A New Algorithm for Crack Localization in a Rotating Timoshenko Beam

AHMAD A. MASOUD
Department of Electrical Engineering, King Fahd University of Petroleum & Minerals, P.O. Box 287, Dhahran 31261, Saudi Arabia

SAMER AL-SAID
Department of Mechanical Engineering, King Saud University, P.O. Box 800, Riyadh 11421 Riyadh, Kingdom of Saudi Arabia (masoud@just.edu.jo.)

Abstract: In this paper a new crack localization algorithm based on a mathematical model describing the lateral vibration of a rotating cracked Timoshenko beam is proposed. The Lagrange equation and the assumed mode method are used to derive the model. The localization algorithm utilizes the variation in a single natural frequency of the beam versus a few rotor speed values to detect and localize a crack. The algorithm has different means of checking/reconfirming its crack estimate. This may be used to improve the accuracy of the decision. Also, the effect of rotational speed and crack location on the system's dynamical characteristics is investigated using the derived mathematical model. The results are compared with those obtained from a three-dimensional finite-element analysis. Good agreement is observed between the two sets of results. Finally, the reliability of the identification algorithm is established using the data obtained from the finite-element analysis.

1. INTRODUCTION

During the last two decades, the focus of many researchers was on improving damage-revealing techniques for vibrating structures such as aircraft structures, large space structures and structures used in an ocean environment. Damage in the form of cracks can occur in structures owing to their limited fatigue strengths. It could also result from the manufacturing process. During structural vibration these cracks may grow over time to a level where they could pose a threat to the integrity of the structure. Therefore, they should be located and repaired at an early stage before they propagate and harm the structure. It has been reported in the literature that a crack does change the dynamical characteristics of a system. It is also considered to be one of the parameters for mode localization in a blade-disk or a periodic system. In these systems, a crack significantly affects the vibrational modes by changing them from the uniform modes to the localized modes. Such mode localization may, in turn, confine the vibrational energy in the vicinity of the cracked blade. Owing to the large cyclic

fatigue generated during operation, the interaction between this localized vibration and the propagation of the crack may cause the blade to fatally fail.

There are several techniques for nondestructive testing available for crack detection, such as visual examination, radiographic tests, ultrasonic testing, liquid penetration tests, X-rays test and magnetic particle tests. These methods are costly and cannot be utilized while the structure is in operation. Owing to these limitations it is now believed that the monitoring of the global dynamics of structures offers a promising alternative for damage detection.

The fact that a crack or a local defect affects the dynamical response of a structure is well known. The modal parameters such as natural frequencies and mode shapes can be used to discover the initiation and growth of fatigue-induced cracks. Numerous attempts to quantify local defects have been reported in the literature. Several researchers utilize the changes in the system's dynamical behavior as a diagnostic tool for damage detection in beams. The motivation for this is the identification of cracks in a beam, which provides a point of reference to test the accuracy of the proposed identification techniques. Also, many mechanical systems have dynamic behavior similar to a single beam (e.g. shafts, blades and robot arms). Several authors (e.g. Wauer, 1990; Dimarogonas, 1996; Doebling et al., 1998; Chasalevris and Papadopoulos, 2006) have presented comprehensive state-of-the-art reviews on the subject. These papers provide a two-decade review of the structural crack detection methods, which utilize the changes in a structure's dynamical characteristics. In the following, additional work concerning the vibration of a cracked Timoshenko beam is reviewed.

Mei et al. (2006) used the wave propagation approach to study free and forced vibration of an axially loaded cracked Timoshenko beam. They derived transmission and reflected matrices for different types of beam faults such as cracks, flexible boundaries and changes in beam section. The effects of crack depth, location, axial load and step section change on the dynamical characteristics of a Timoshenko beam were investigated numerically.

Masoud et al. (1998) derived a mathematical model describing the lateral vibration of a fixed–fixed cracked beam under constant axial loading using modal analysis. They also studied the interaction between the crack depth and axial load, and the effect of this interaction on the natural frequencies of the system. The theoretical results obtained were verified experimentally.

Fang et al. (2006) developed analytical solutions describing free and forced vibrations of a bladed-disk system with a single cracked blade. A simple system of Euler–Bernoulli cantilevered beams (blades) connected by springs was used. The effect of a crack on the system dynamical characteristics was investigated showing that even for a small crack, vibration mode localization and forced response localization are present.

Kuang and Huang (1999) conducted a similar study where they used the Galerkin method to derive the equation of motion for a rotating shrouded bladed-disk system with a single blade crack. The blades were modeled as Euler–Bernoulli beams, while the cracked beam was modeled as two-span beam connected with a torsional spring. Numerical solutions were obtained to show the effect of crack depth, location and rotational speed on the dynamic characteristics of the system. The results indicate that blade crack can be considered as a reason for the localization phenomenon found in rotating bladed disks.

Huang (2006) used Hamilton's principle to derive the governing equations of motion for rotating shrouded pre-twisted cracked blades. The discrete equations of motion were solved numerically using the Galerkin method. The Euler–Bernoulli beam model was employed

to characterize the tapered pre-twisted blade. They showed that the number of blades may influence the localization frequency and vibration in the bladed-disk system. The study also revealed that localization modes in the system are significantly affected by the number and the distribution of cracked blades in the mistuned system. Moreover, increasing the number of cracked blades enhances mode localization.

A crack identification technique for a rotating thick blade was proposed by Chang and Chen (2004). Their technique was based on spatial wavelet analysis, where a finite element model was derived to calculate the mode shapes for the rotating cracked blade and these mode shapes were analyzed using the wavelet transform. They showed that the distributions of the wavelet coefficients can identify the crack position.

A finite spectral Timoshenko beam element with a transverse open, nonpropagating crack was proposed by Krawczuk et al. (2003). The crack was simulated by a massless spring that has bending and shear flexibilities which were calculated using Castigliano's theorem and the laws of fracture mechanics. They used the element for beam modal analysis as well as wave propagation analysis. The derived element has the ability to analyze the beam over a very wide range of frequencies. Consequently, high natural frequencies can be calculated simply. This leads to accurate crack detection since very small cracks cause measurable changes in high natural frequencies.

Loya et al. (2006) studied the lateral vibration of a cracked Timoshenko beam. The beam was simulated as two beams connected by extensional and rotational massless springs at the crack location. The beam natural frequencies were found by direct solution for the differential equations of motion. Also a perturbation solution to calculate the system's natural frequencies was derived. A closed form solution was obtained for only a simply supported beam. The work reveals that the perturbation solution has good accuracy only for shallow cracks. Sung-Soo and Ji-Hwan (2003) derived a finite element model for open-cracked and breathing-cracked beams to study the effect of a crack in a rotating cantilever composite beam. Crack location, depth, fiber angle, and volume fractions were studied as a function of rotation speed. The study showed that a crack changes the beam's natural frequencies.

Al-Said et al. (2006) derived a simple mathematical model to describe the lateral vibration of a cracked rotating Timoshenko beam. They used the model to study the effect of crack depth, rotating speed and shear deformation on the beam's natural frequencies. Their study showed that uncertainty exists in determining the reduction in the beam's natural frequencies due to a crack by simply subtracting the frequency of the intact rotating beam from that of the cracked beam. Also, the frequency difference between the cracked Timoshenko beam and the cracked Euler–Bernoulli beam was a monotonically increasing function of the crack's depth. This meant that ignoring the shear effect leads to an underestimation of the frequency change caused by the crack.

Most of the previous work used the Euler–Bernoulli beam model to characterize a cracked beam. Based on this model several crack identification algorithms were proposed. Some of these works present crack identification algorithms that take into account the shear effect, particularly in the case of rotating blades (beam with variable axial load). However, they used finite elements in the modeling where the crack is added as a local flexibility in the global system.

In this work the mathematical model suggested by Al-Said et al. (2006) for describing the lateral vibration of rotating cracked Timoshenko beam (Figure 1) is improved. The
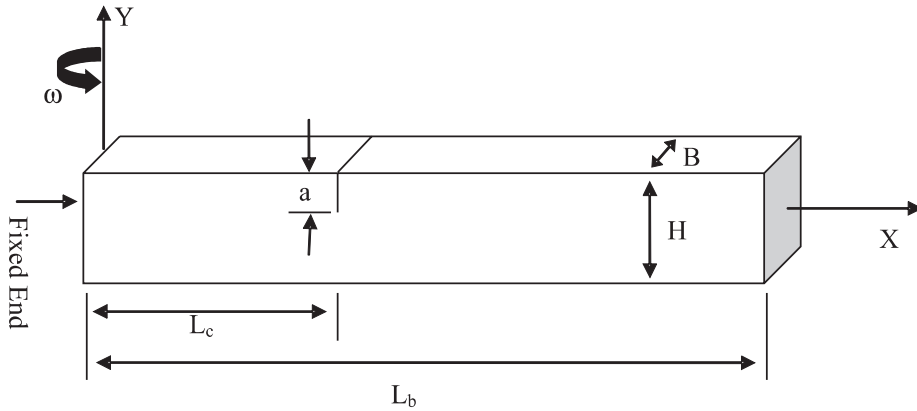
Figure 1. Physical model for the rotating cracked beam.

enhancement is achieved by adding the crack's effect on the beam's lateral deformation in addition to its effect on the beam slope. Also a more accurate function describing the stress intensity factors corresponding to the first and the second modes of crack growth is adopted. The assumed mode method combined with Lagrange's equation is used to derive the governing equations of motion for the system. Using this method in the derivation reflects the crack and the rotational speed effects in all system modes. Therefore, these effects globally manifest their presence throughout the system.

In practice the changes to the system's dynamical characteristics, which are used to identify cracks, may be measured globally. Therefore, using the aforementioned method to derive the mathematical model that describes the system's dynamical behavior will match up with the actual procedures used to measure the system's dynamical parameters. The model is verified by means of three-dimensional finite-element model analysis. The general purpose finite-element program ANSYS 8.0 is used. The derived model is used as a basis for a new crack localization algorithm that utilizes the variation of a single natural frequency versus a few values of rotational speed to identify the location of the crack. The proposed algorithm has different means of checking/reconfirming its crack estimates. This may be used to improve the accuracy of the decision. This is achieved by utilizing different combinations of rotational speeds and natural frequency variations. The finite-element analysis (FEA) is used to check the capability and the accuracy of the algorithm in identifying crack location.

NOMENCLATURE

D Crack depth ratio (a/H)
E Modulus of elasticity
G Shear modulus
I Area moment of inertia
J Beam mass moment of inertia per unit length $J = \rho I = m_b K^2$
K Cross-section radius of gyration

L_b Beam length

m_b Mass per unit length of the beam

M Internal beam moment

T, U Beam kinetic and potential energy, respectively

t^* Reference time, $= \sqrt{\dfrac{\rho A L_b^4}{EI}}$

y Total beam deflection

η Beam cross-sectional angle of distortion due to shear

κ Cross-section shear factor.

ψ Beam cross-section angel of rotation due to bending

Θ_b Dimensionless crack flexibility due to bending moment

Θ_s Dimensionless crack flexibility due to shear force

ω Angular speed

τ Dimensionless time, $= \dfrac{t}{t^*}$

ξ Dimensionless coordinate, $= \dfrac{x}{L_b}$

U_1 Inertia parameter, $= \dfrac{K^2}{L_b^2}$

U_2 Shear parameter; $= \dfrac{\kappa G}{EI}$

U_3 Beam depth to length ratio, $= \dfrac{H}{L_b}$

f_i, q_i ith generalized coordinate for total deflection and pure bending

Y_i, Ψ_i ith mode shape for total deflection and pure bending

Ω Dimensionless angular speed

$\beta_{\Omega,c}$ Non-dimensional natural frequency of rotating cracked beam

β_{Ω} Non-dimensional natural frequency of rotating intact beam

$\omega_{\Omega,c}$ Dimensional natural frequency of rotating cracked beam

ω_{Ω} Dimensional natural frequency of rotating intact beam

$\omega_{0,0}$ Dimensional natural frequency of non-rotating intact beam

$(\dot{\ })$ Total derivative with respect to

2. MATHEMATICAL MODELING

In this section a mathematical model describing the lateral vibration of rotating cracked cantilever Timoshenko beam with a uniform rectangular cross section is developed. The beam is assumed to rotate in the horizontal (x–z plane) at a constant angular speed (ω) with a single sided crack (Figure 1). The cracked beam is simulated using two uniform Timoshenko beams connected by two massless torsional and translational springs to take into account the rotational and translational discontinuities in the beam's deflection at the crack location (Figure 2a).
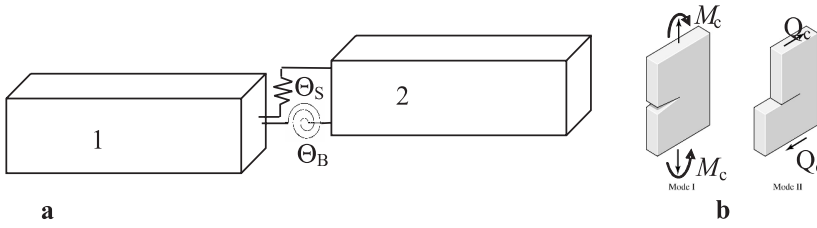
Figure 2. Mathematical model: (a) cracked beam; (b) fracture modes.

Rotation of the beam about an axis produces variable axial load due to centrifugal force:

$$P(x,t) = \int_x^{L_b} m_b \omega^2 \zeta \, d\zeta = \frac{1}{2} m_b \omega^2 L_b^2 \left(1 - \frac{x^2}{L_b^2}\right). \tag{1}$$

The beam is assumed to have a uniform cross-section area (A), mass per unit length (m_b), area moment of inertia (I) and constant modulus of elasticity (E). The total deflection $y(x,t)$ of the beam at any point (x) consists of two parts: the first is caused by pure bending and the second is caused by pure shear. Therefore, the slope of the deflection curve ($y(x)$) may be written as

$$\frac{\partial y}{\partial x} = \psi(x,t) + \eta(x,t), \tag{2}$$

where $\psi(x,t)$ is the angle of rotation due to bending and $\eta(x,t)$ is the angle of distortion due to shear. The transverse and angular deflections are assumed to be small. The relation between the bending moment (M) and the bending rotation $\psi(x,t)$ is

$$M(x,t) = EI\frac{\partial \psi}{\partial x}. \tag{3}$$

The relation between the shearing force (Q) and shear angle $\eta(x,t)$ is

$$Q(x,t) = \kappa G A \eta(x,t) \tag{4}$$

where κ is the shear coefficient (Cowper, 1966). To write the equation of motion governing the vibration of a rotating cracked Timoshenko beam, the Lagrange's method and the assumed mode method are adopted. This approach makes it possible to globalize the effects of both the crack and the rotational speed on the dynamical characteristics of the beam.

The kinetic energy of the beam is obtained as the summation of translatory and rotary inertia effects:

$$T = \frac{1}{2} \int_0^{L_b} m_b \left(\frac{\partial y(x,t)}{\partial t}\right)^2 dx + \frac{1}{2} \int_0^{L_b} J \left(\frac{\partial \psi(x,t)}{\partial t}\right)^2 dx. \tag{5}$$

The strain energy U of the beam due to elastic bending, shear deformation, variable axial force and the crack is

$$
U = \frac{1}{2} \int_0^{L_b} EI \left(\frac{\partial \psi}{\partial x} \right)^2 dx + \frac{1}{2} \int_0^{L_b} \kappa GA \left(\frac{\partial y}{\partial x} - \psi \right)^2 dx
$$

$$
+ \int_0^{L_b} P(x,t)(ds - dx) + \Pi_c, \tag{6}
$$

$$
\Pi_c = \frac{1}{E} \int_{A_c} \left(K_I^2 + K_{II}^2 \right) dA_c. \tag{7}
$$

The term $(ds - dx)$, represents the change in the horizontal projection of an element of length (ds):

$$
ds - dx = \left\{ (dx)^2 + \left[\frac{\partial y(x,t)}{\partial x} \right]^2 (dx)^2 \right\}^{1/2} - dx \cong \frac{1}{2} \left[\frac{\partial y(x,t)}{\partial x} \right]^2 dx \tag{8}
$$

where A_c is the crack area, K_I and K_{II} are the stress intensity factors corresponding to the first and the second mode of crack growth (Tada et al., 2000) which are calculated as follows:

$$
K_I = \frac{6M_c}{B \times H^2} \sqrt{\pi H \times D} F_I(D), \quad K_{II} = \frac{Q_c}{B \times H} \sqrt{\pi H \times D} F_{II}(D)
$$

$$
F_I(D) = \sqrt{\frac{\tan(0.5\pi D)}{0.5\pi D}} \frac{0.923 + 0.199(1 - \sin(0.5\pi D))^4}{\cos(0.5\pi D)}
$$

$$
F_{II}(D) = \frac{1.122 - 0.561D + 0.085D^2 + 0.18D^3}{\sqrt{1 - D}}
$$

where M_c, Q_c are the bending moment and shear force at crack location respectively (Figure 2b) where $D = a/H$, a is the crack depth, H is the beam depth and B is the beam width.

The assumed mode method is an approximate numerical method in which a solution is assumed in the form of a linear superposition of admissible functions $Y(x)$, $\Psi(x)$, and a generalized coordinates, $q(t)$, $f(t)$:

$$
y(x,t) = \sum_{i=1}^{n} Y_i(x) q_i(t), \qquad \psi(x,t) = \sum_{i=1}^{n} \Psi_i(x) f_i(t) \tag{9}
$$

where $Y_i(x)$ is the ith total deflection, $\Psi_i(x)$ is the ith angle of rotation due to pure bending for the beam, q_i and f_i are the ith generalized total deflection and pure bending coordinates, respectively. To find the general governing equations of motion, the beam's kinetic (T) and strain (U) energies are substituted in Lagrange's equation:

$$\frac{\partial}{\partial t}\left(\frac{\partial T}{\partial \dot{b}_i}\right) - \frac{\partial T}{\partial b_i} + \frac{\partial U}{\partial b_i} = 0. \tag{10}$$

Using y and ψ as defined in Equation (9), the kinetic and strain energies (Equations (5) and (6)) may be written as follows:

$$T = \frac{1}{2}\int_0^{L_b} m_b \sum_{i=1}^n \sum_{j=1}^n \dot{q}_i \dot{q}_j Y_i Y_j dx + \frac{1}{2}\int_0^{L_b} J \sum_{i=1}^n \sum_{j=1}^n \dot{f}_i \dot{f}_j \Psi_i \Psi_j dx \tag{11}$$

$$U = \frac{1}{2}\int_0^{L_b} EI \sum_{i=1}^n \sum_{j=1}^n f_i f_j \Psi_i' \Psi_j' dx$$

$$+ \frac{1}{2}\int_0^{L_b} \kappa G A \sum_{i=1}^n \sum_{j=1}^n \left(q_i Y_i' - f_i \Psi_i\right)\left(q_j Y_j' - f_j \Psi_j\right) dx$$

$$+ \int_0^{L_b} P(x) \sum_{i=1}^n \sum_{j=1}^n q_i q_j Y_i' Y_j' dx + 48\pi\, EI \frac{H}{L^2}\Theta_b \sum_{i=1}^n \sum_{j=1}^n f_i f_j \Psi_i' \Psi_j'\Big|_{x_c}$$

$$+ \pi\kappa^2 H^2 \times B\frac{G^2}{E}\Theta_s \sum_{i=1}^n \sum_{j=1}^n \left(q_i Y_i' - f_i \Psi_i\right)\left(q_j Y_j' - f_j \Psi_j\right)\Big|_{x_c} \tag{12}$$

where

$$\Theta_b = \int_0^D DF_I^2(D)dD, \quad \Theta_s = \int_0^D DF_{II}^2(D)dD. \tag{13}$$

Substituting Equations (11) and (12) into Lagrange's equation (10), the coupled equations describing the flexural vibration of a rotating cracked Timoshenko beam are obtained. These equations are written in the nondimensional form:

$$\mathbf{M}_{2n\times 2n}\left\{\begin{array}{c}\ddot{\mathbf{q}}_{nx1}\\ \ddot{\mathbf{f}}_{nx1}\end{array}\right\} + \left[\mathbf{K}_{2n\times 2n} + \Theta_s\mathbf{\Delta K}_{2n\times 2n}\right]\left\{\begin{array}{c}\mathbf{q}_{nx1}\\ \mathbf{f}_{nx1}\end{array}\right\} = \{\mathbf{0}\} \tag{14}$$

where

$$\mathbf{M} = \begin{bmatrix}\int_0^1 Y_r Y_j d\xi & 0 \\ 0 & U_1\int_0^1 \Psi_r \Psi_j d\xi\end{bmatrix}_{2n\times 2n}$$

$$\mathbf{K} = \frac{U_2}{U_1} \begin{bmatrix} \int\limits_0^1 Y_r' Y_j' d\xi + \frac{U_1 \Omega^2}{2U_2} \int\limits_0^1 \left(1 - \xi^2\right) Y_r' Y_j' d\xi & -\int\limits_0^1 Y_j' \Psi_r d\xi \\ -\int\limits_0^1 Y_r' \Psi_j d\xi & \frac{U_1}{U_2} \int\limits_0^1 \Psi_r' \Psi_j' d\xi + \int\limits_0^1 \Psi_r \Psi_j d\xi \end{bmatrix}_{2n \times 2n}$$

$$\mathbf{\Delta K} = 2\pi \frac{U_3 U_2^2}{U_1} \begin{bmatrix} Y_r' Y_j' & -Y_j' \Psi_r \\ -Y_r' \Psi_j & \Psi_r \Psi_j + 18 \left(\frac{U_1}{U_3 U_2}\right)^2 \frac{\Theta_b}{\Theta_s} \Psi_r' \Psi_j' \end{bmatrix}_{2n \times 2n} \bigg|_{\xi_c}.$$

Equation (14) is a system of second-order linear differential equations with constant coefficients. The solution of this system of equations is a typical eigenvalue problem.

3. THE ASSUMED FUNCTION

To obtain a good approximate solution for the above system, the eigenfunctions of a non-rotating cracked Timoshenko beam are used as the assumed functions. Since the crack has a localized effect, the beam is treated as two uniform segments connected by torsion and transverse translational springs at the crack location (Figure 2a). The left segment of the beam is designated by subscript (1), and the right segment by subscript (2). Assuming that the beam is nonrotating and its motion is simple and harmonic, the governing deferential equations of motion in the nondimensional form are

$$\frac{U_2}{U_1} \frac{d^4 Y_i}{d\xi^4} + \lambda^2 \left(1 + U_2\right) \frac{d^2 Y_i}{d\xi^2} - \lambda^2 \left(\frac{U_2}{U_1} - \lambda^2 U_1\right) Y_i = 0, \tag{15}$$

$$\frac{U_2}{U_1} \frac{d^4 \Psi_i}{d\xi^4} + \lambda^2 \left(1 + U_2\right) \frac{d^2 \Psi_i}{d\xi^2} - \lambda^2 \left(\frac{U_2}{U_1} - \lambda^2 U_1\right) \Psi_i = 0. \tag{16}$$

The solutions of these equations are found to be

$$Y_i\left(\xi\right) = C_{1i} \cos \alpha\xi + C_{2i} \sin \alpha\xi + C_{3i} \cosh \gamma\xi + C_{4i} \sinh \gamma\xi, \tag{17}$$

$$\Psi_i\left(\xi\right) = A_{1i} \cos \alpha\xi + A_{2i} \sin \alpha\xi + A_{3i} \cosh \gamma\xi + A_{4i} \sinh \gamma\xi, \tag{18}$$

$$A_{1i} = \frac{1}{\alpha} \left(\alpha^2 - \frac{U_1}{U_2}\lambda^2\right) C_{2i}, \quad A_{2i} = -\frac{1}{\alpha} \left(\alpha^2 - \frac{U_1}{U_2}\lambda^2\right) C_{1i},$$

$$A_{3i} = \frac{1}{\gamma} \left(\gamma^2 + \frac{U_1}{U_2}\lambda^2\right) C_{4i}, \quad A_{4i} = \frac{1}{\gamma} \left(\gamma^2 + \frac{U_1}{U_2}\lambda^2\right) C_{3i},$$

$$\alpha = \lambda\sqrt{0.5}\left[\frac{U_1}{U_2} + U_1 + \sqrt{\left(\frac{U_1}{U_2} + U_1\right)^2 - 4\left(\frac{U_1^2}{U_2}\right) - \frac{4}{\lambda^2}}\right]^{0.5},$$

$$\gamma = \lambda\sqrt{0.5}\left[-\frac{U_1}{U_2} - U_1 + \sqrt{\left(\frac{U_1}{U_2} + U_1\right)^2 - 4\left(\frac{U_1^2}{U_2}\right) - \frac{4}{\lambda^2}}\right]^{0.5}.$$

In order to find the coefficients of each function Y and Ψ as well as the constants γ and α, the case of a clamped free beam is considered. The boundary conditions applied to the clamped end are

$$Y_1(0) = 0, \quad \Psi_1(0) = 0.$$

At the crack location the compatibility of both moment and shear force are assured by applying the following conditions:

$$\Psi_1'(\xi_c) = \Psi_2'(\xi_c), \quad Y_1'(\xi_c) - \Psi_1(\xi_c) = Y_2'(\xi_c) - \Psi_2(\xi_c).$$

At a crack location, the beam's displacement and slope are discontinuous (Figure 2b). This is due to the additional flexibility introduced by the crack. As a result the following displacement and slope conditions are held at crack location:

$$Y_1(\xi_c) + 2\pi U_2 U_3 \Theta_s \left(Y_1'(\xi_c) - \Psi_1(\xi_c)\right) = Y_2(\xi_c),$$

$$\Psi_1(\xi_c) + 2\pi \frac{36 U_1}{U_3} \Theta_b \Psi_2'(\zeta_c) = \Psi_2(\xi_c).$$

Finally, at the free end of the beam, the moment and shear force vanish leading to

$$\Psi_2'(1) = 0, \quad Y_2'(1) - \Psi_2(1) = 0.$$

Substituting Equations (17) and (18) into the above boundary conditions for the cantilever beam, we obtain eight linear algebraic homogenous equations. These equations may be written in a matrix form as

$$[A]_{8\times8} \{C\}_{8\times1} = \{0\}.$$

To calculate the natural frequencies of the nonrotating cracked beam, the determinant of $[A]$ is set to zero. The corresponding coefficient vector $\{C\}$ is calculated. The resulting frequencies and coefficients are substituted into Equations (17) and (18) to determine the mode shapes for total deflection of the cracked beam $(Y(\xi))$ and the beam's slope due to pure bending $(\Psi(\xi))$. These functions are substituted into Equation (14) to find the governing equations of motion for a rotating cracked Timoshenko beam.

4. IDENTIFICATION ALGORITHM

Since the beam deflection is a simple harmonic motion, the nondimensional differential equation is represented in the following eigenvalue problem format:

$$\left[- \left(\beta_{\Omega c}^i \right)^2 \mathbf{M} + \mathbf{K} + \Theta_s \Delta \mathbf{K} \right] \mathbf{Q}_{\Omega c}^i = \{\mathbf{0}\}, \tag{19}$$

where the elements of matrix $\Delta \mathbf{K}$ are the variation of the system stiffness due to the crack only, and $\beta_{\Omega c}^i$ is the ith nondimensional natural frequency of the system. The above equation is reduced to represent the lateral vibration of the intact system. By setting the crack flexibilities Θ_s and Θ_b to zero:

$$\left[- \left(\beta_{\Omega}^i \right)^2 \mathbf{M} + \mathbf{K} \right] \mathbf{Q}_{\Omega}^i = \{\mathbf{0}\}. \tag{20}$$

Substitute the mass matrix in Equation (19) by its value obtained from Equation (20), the crack shear flexibility can be obtained in terms of the intact and cracked system dynamic characteristics as

$$\begin{aligned} \Theta_s(D) &= \Gamma^i(\xi, D, \Omega) \\ \Gamma^i &= \frac{(\beta_{\Omega c}^i)^2 - (\beta_{\Omega}^i)^2}{(\beta_{\Omega}^i)^2} \times \frac{\mathbf{Q}_{\Omega}^{i\,\mathrm{T}} \mathbf{K} \mathbf{Q}_{\Omega c}^i}{\mathbf{Q}_{\Omega}^{i\,\mathrm{T}} \Delta \mathbf{K} \mathbf{Q}_{\Omega c}^i} \end{aligned} \tag{21}$$

where Γ^i is called the ith mode equivalent crack flexibility. From this equation it can be seen that Θ_s is crack depth-dependant only (Equation (13)) and its value is constant for any rotor speed and system vibrational modes. The steps to predict a crack location are as follows. A single mode natural frequency of the intact beam is measured for a few rotational speeds. The same natural frequencies at the same rotational speeds are monitored. If variations are noticed, a crack may have started to form. The two measured sets of natural frequencies are substituted into Equation (21). Plotting the value of Γ^i for a single vibrational mode (e.g. the first mode) at few rotational speeds versus beam span (ξ) yields curves that intersect at a single point. This point is the crack location. In practice, the mode frequency values, β_{Ω} and $\beta_{\Omega c}$, are found experimentally with some measuring error. Therefore, Γ^i curves will not intersect at a single point; instead, they will intersect within a small region. To simplify the crack position search, an ith mode distance function $\sigma_i(\xi)$ is defined as

$$\begin{aligned} \sigma_i(\xi) = \ & \frac{1}{N} \left[\left| \Gamma^i(\xi, D, \Omega_1) - \Gamma^i(\xi, D, \Omega_N) \right| \right. \\ & + \left. \sum_{j=1}^{N-1} \left| \Gamma^i(\xi, D, \Omega_j) - \Gamma^i(\xi, D, \Omega_{j+1}) \right| \right]. \end{aligned} \tag{22}$$

Theoretically, this function is equal to zero at the crack location. In practice, this function has a minimum value at the crack location.
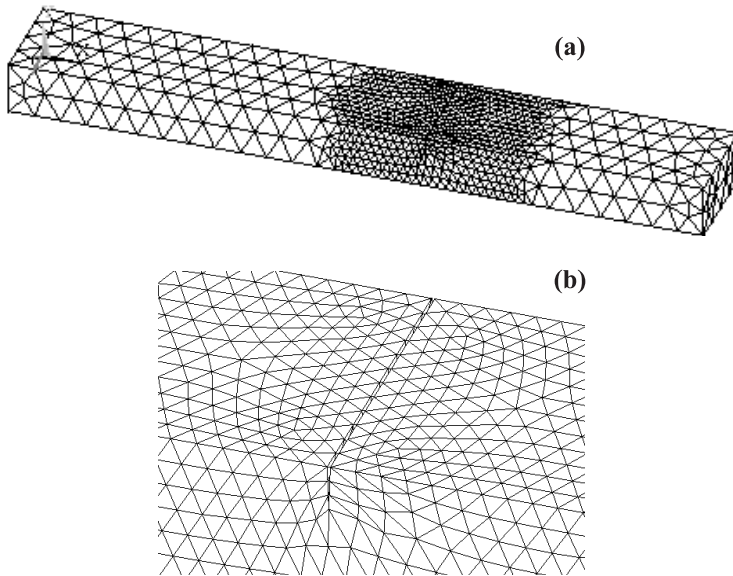
Figure 3. Finite-element model: (a) three-dimensional mesh for the cracked beam; (b) meshing layout near the crack.

Two methods are usually used to verify the reliability of the proposed mathematical model and the identification algorithm. The first one is experimental and the second is based on finite element analysis. In this work, finite element analysis is considered as a method of verification, since it provides a simple way to generate as many check points as desired. Three-dimensional FEA is carried out using the commercial software ANSYS 8.0 to verify the results obtained from the proposed mathematical model. In the three-dimensional FEA a 10-node tetrahedral element type is used to model a clamped–free rotating beam. The crack is represented by a sharp V-notch. A nonuniform mesh with very fine tessellation in the vicinity of the crack is used in the modeling (Figure 3). Also, a convergence test is applied to the first four natural frequencies of the beam to ensure high-precision results.

5. RESULTS AND DISCUSSION

A simple crack localization algorithm is proposed utilizing the variation of a single system natural frequency versus a beam's rotational speed. The algorithm is based on a mathematical model describing the lateral vibration of a rotating cracked Timoshenko beam.

The effect of shear deformation, rotational speed and crack depth were investigated thoroughly by Al-Said et al. (2006); however, this work focuses on demonstrating the ability of the proposed crack localization algorithm to detect a crack at different crack locations.

To verify the accuracy of the derived mathematical model in predicting the system's frequencies, the first three beam natural frequencies versus its rotational speeds are calculated using the proposed model. The results are compared with those obtained from the FEA.
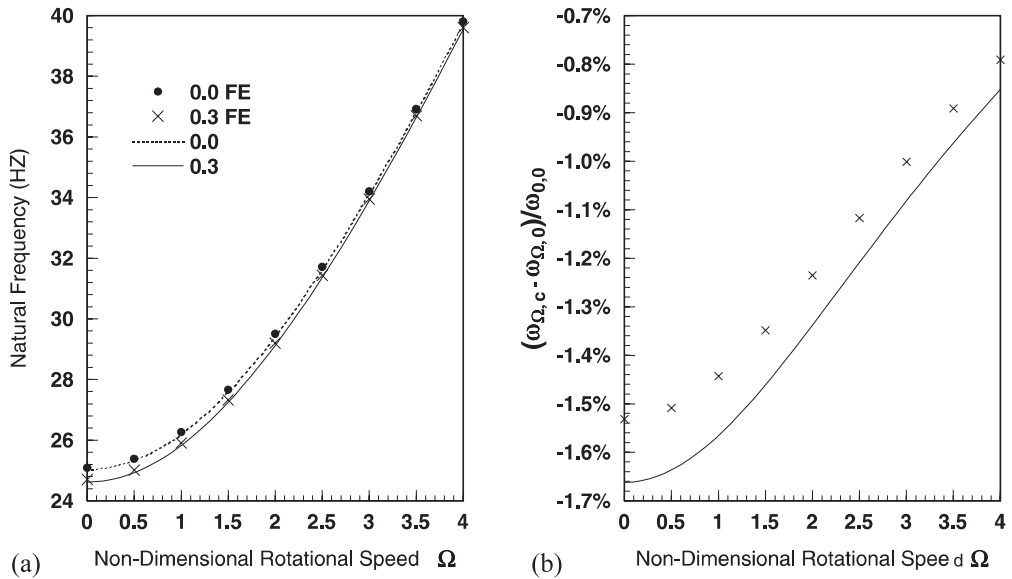
Figure 4. First natural frequency versus rotational speed (L_b = 0.7 m, ξ_c = 0.25): (a) absolute frequency; (b) frequency change ratio.

Only the first three modes (n =3) are used to compute the beam's deflection (y) and bending (ψ) assumed functions described in Equation (9). As a result, the system of equations governing the lateral vibration of the rotating cracked Timoshenko beam (Equation (14)) has a dimensionality equal to 6 × 6. The mathematical model is tested for a long steel beam (E = 200 GPa, v = 0.3 ρ = 7800 Kg/m³, low shear effect) with the following dimensions, L_b = 0.7 m, H = 0.015 m, B = 0.03 m and has a crack at ξ_c = 0.25 with depth D = 0.3. Figure 4(a) shows that the first natural frequency of the system is proportional to the rotating speed for both cracked and intact beams. Also, Figure 4(b) shows that by increasing the rotor's speed the frequency change due to the crack decreases. The figures also reveal that the FEA results highly match the theoretical results.

Comparable results are obtained for the natural frequencies of the second and the third system as shown in Figures 5 and 6, respectively. The mathematical model is also tested for a short beam. The beam has properties similar to those of the previous model except its length, L_b = 0.2 m. Figures 7, 8 and 9 show the variation of the natural frequencies of the first, second and third system for the short beam versus the beam's rotational speeds, respectively. The figures reveal similar behavior to the long beam results. Also the close matching between the FEA results and the results obtained from the mathematical model is observed.

The effect of a crack location (ξ_c) on the first three system natural frequencies is investigated. This is used to explore the accuracy of the mathematical model in predicting these frequencies for different crack locations. Since this work deals with a Timoshenko beam, the results for the short beam are used to derive the following conclusions. Figure 10a shows the variation of the first system natural frequency versus the crack location as a function of the
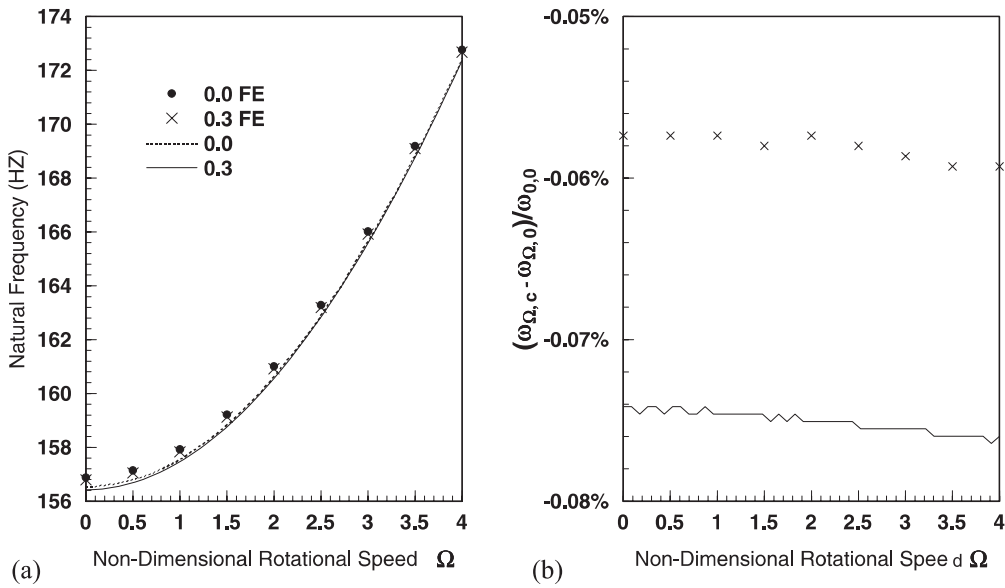
Figure 5. Second natural frequency versus rotational speed ($L_b = 0.7$ m, $\xi_c = 0.25$): (a) absolute frequency; (b) frequency change ratio.
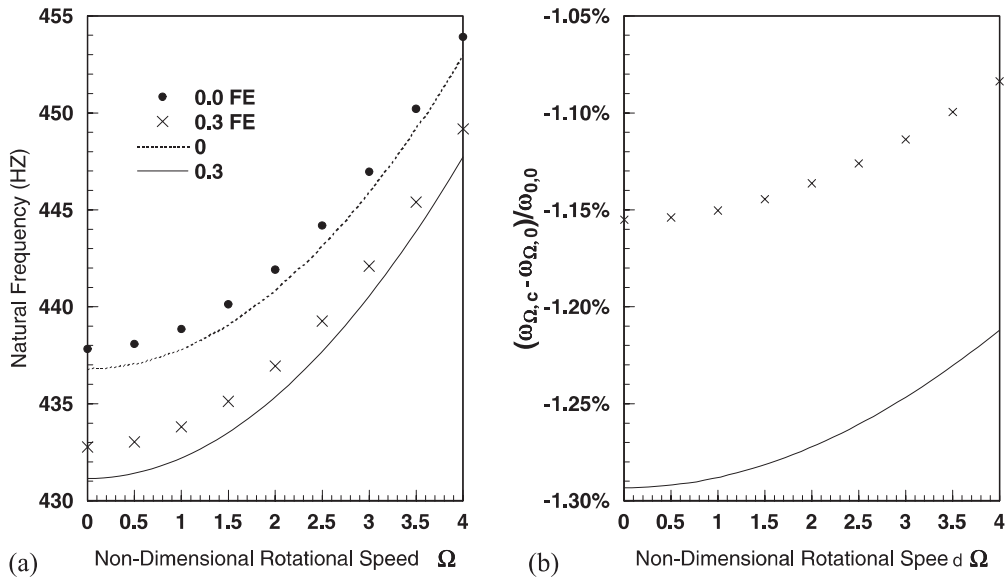

Figure 6. Third natural frequency versus rotational speed ($L_b = 0.7$ m, $\xi_c = 0.25$): (a) absolute frequency; (b) frequency change ratio.
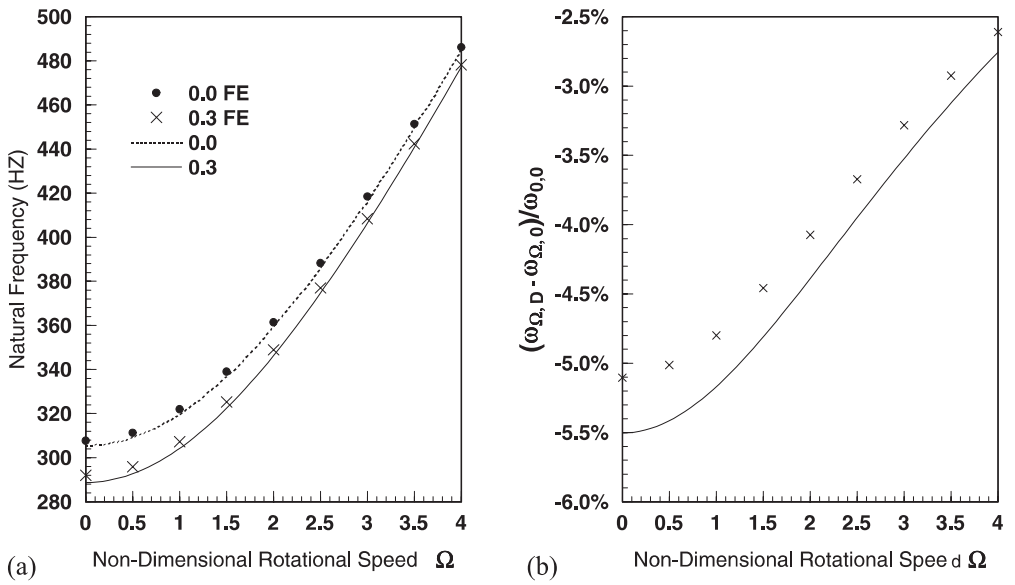
Figure 7. First natural frequency versus rotational speed ($L_b = 0.2$ m, $\xi_c = 0.25$): (a) absolute frequency; (b) frequency change ratio.
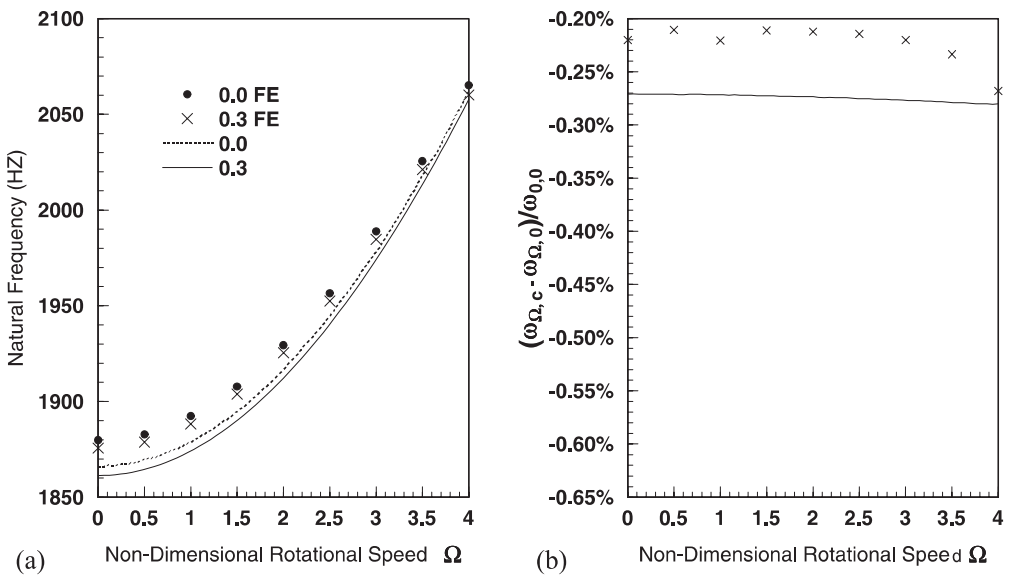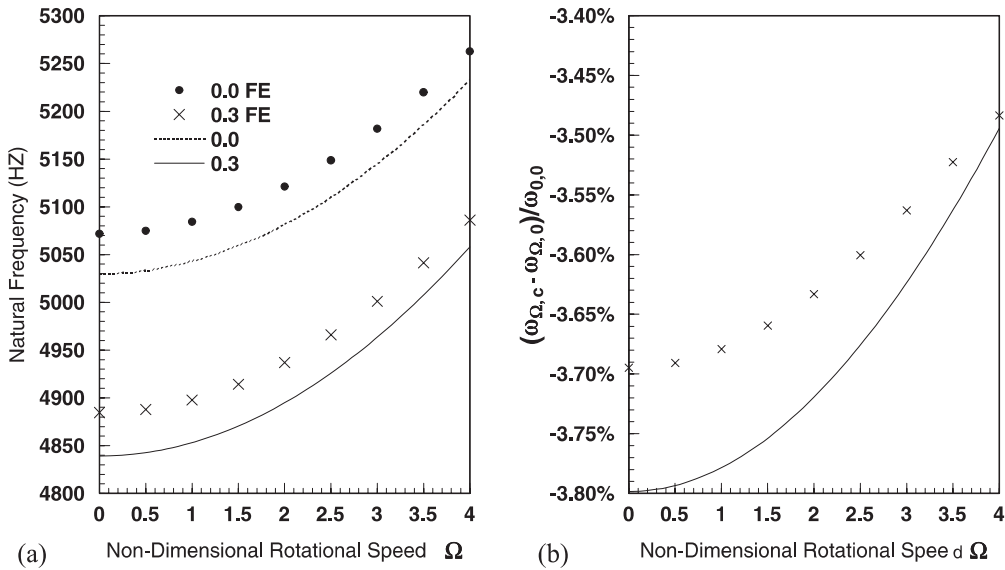

Figure 8   Second natural frequency versus rotational speed ($L_b = 0.2$ m, $\xi_c = 0.25$): (a) absolute frequency; (b) frequency change ratio.

Figure 9. Third natural frequency versus rotational speed (L_b = 0.2 m, ξ_c = 0.25): (a) absolute frequency; (b) frequency change ratio.
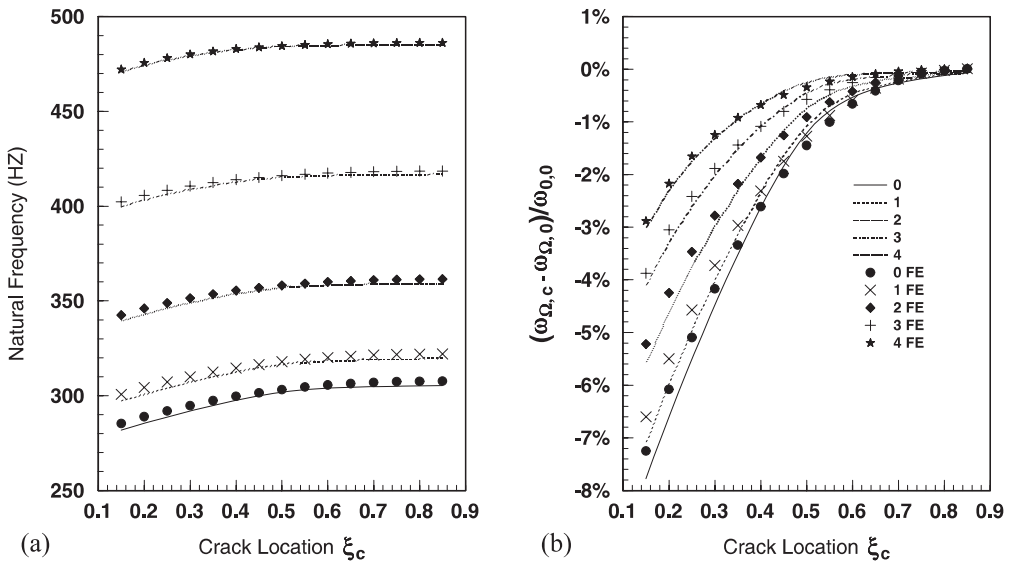

Figure 10. First natural frequency versus crack location in terms of rotational speed Ω (L_b = 0.2 m, D = 0.3): (a) absolute frequency; (b) frequency change ratio.

Figure 11. Second natural frequency versus crack location in terms of rotational speed Ω ($L_b = 0.2$ m, $D = 0.3$): (a) absolute frequency; (b) frequency change ratio.

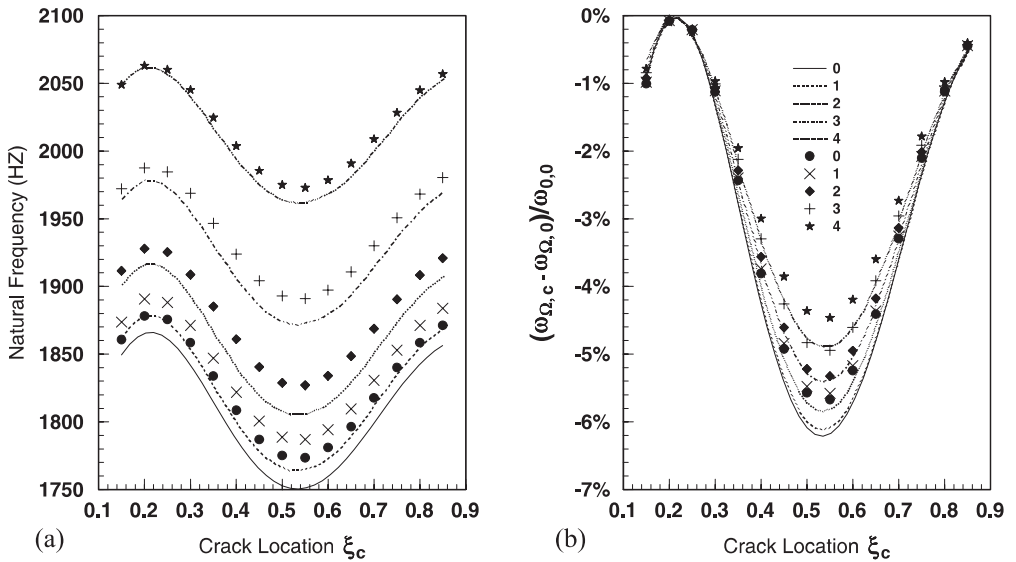rotation speed. It can be seen that moving the crack away from the beam's root leads to an increase in the natural frequency. This is clearly shown in Figure 10b, where the frequency difference (the frequency of the cracked beam minus the frequency of the intact beam) approaches zero when the crack location approach the beam's tip. This is observed for all rotational speeds. This result is expected since moving the crack away from the beam's root places it in a position that has low curvature. As a result the influence and the natural frequency of the crack decrease. In Figures 10a and 10b the FEA results show a similar trend and high agreement with their theoretical counterparts.

The variation of the second system natural frequency versus the crack location is demonstrated in Figure 11a. The maximum reduction is observed around the mid-span crack location. However, moving the crack away from the beam's mid-span leads to less reduction in the natural frequency. These results are observed for all rotational speeds shown in Figure 11b, where the frequency difference is plotted versus the crack location. This may be justified by noticing that the maximum beam curvature is approximately located near the mid-span in the case of the second mode vibration. As a result the crack strength will be at its highest. On the other hand, the curvature decreases away from this location causing the effect of the crack to weaken. The FEA results are also shown in these two figures. It can be seen that these results match well the theoretical results.

The third system natural frequency variation versus crack location is shown in Figure 12 for different values of rotational speeds. Figure 12 reveals that the frequency will fluctuate depending on the crack location. This fluctuation is also observed in the FEA results which accurately match-up with the theoretical results. Figure 12 shows that the maximum reductions in the frequency occur where the crack is around $\xi_c = 0.3$ and 0.7. These two locations have the maximum curvatures in the case of the third mode vibration.
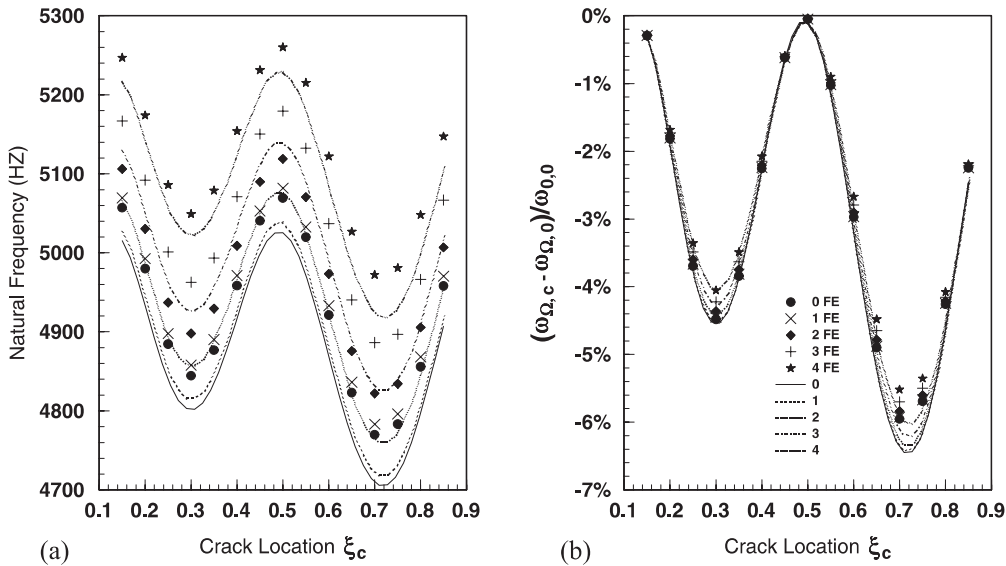
Figure 12. Third natural frequency versus crack location in terms of rotational speed Ω ($L_b = 0.2$ m, $D = 0.3$): (a) absolute frequency; (b) frequency change ratio.

In all of these figures the high matching between the theoretical results and the FEA results strengthen the confidence in the ability of the derived mathematical model to accurately predict the system natural frequencies for a rotating cracked Timoshenko beam. Also, one must keep in mind that the finite-element model (which is used to verify the theoretical results) is three-dimensional and the crack is introduced as a sharp v-notch which closely simulates a real physical crack (Figure 3).

Since the fidelity of the mathematical model is established, it is introduced into the crack localization algorithm (described in Section 4) to predict the location of a crack. A crack is introduced into the finite-element model. The frequency reduction due to the crack is calculated for a few values of rotational speeds. The FEA results are used to substitute for the measured experimental data used by the algorithm to estimate the crack location placed in the finite-element model. The advantage of this algorithm compared with the existing models found in literature is that only one single natural frequency variation needs to be monitored versus a few rotational speeds. Therefore, the first system natural frequency variation (between the intact beam and a beam with crack depth $D = 0.3$) is found for four rotational speeds namely $\Omega = 1, 2, 3, 4$. Different combinations of these frequency variations are used to evaluate the first mode distance function $\sigma_1 (\xi)$ in order to predict the crack location.

Figure 13a shows the $\sigma_1 (\xi)$ function versus the beam span for different crack locations using the four values of the rotational speeds $\Omega = 1, 2, 3, 4$. Figure 13a shows that the distance function ($\sigma_1 (\xi)$) has its minimum at the beam's span location which lies in the vicinity to the actual crack. An isolated failure to predict the crack's location is observed for $\xi_c = 0.15$. In all remaining cases the distance function provides an accurate prediction of the crack location with a detection estimate very close to the real location. Using three
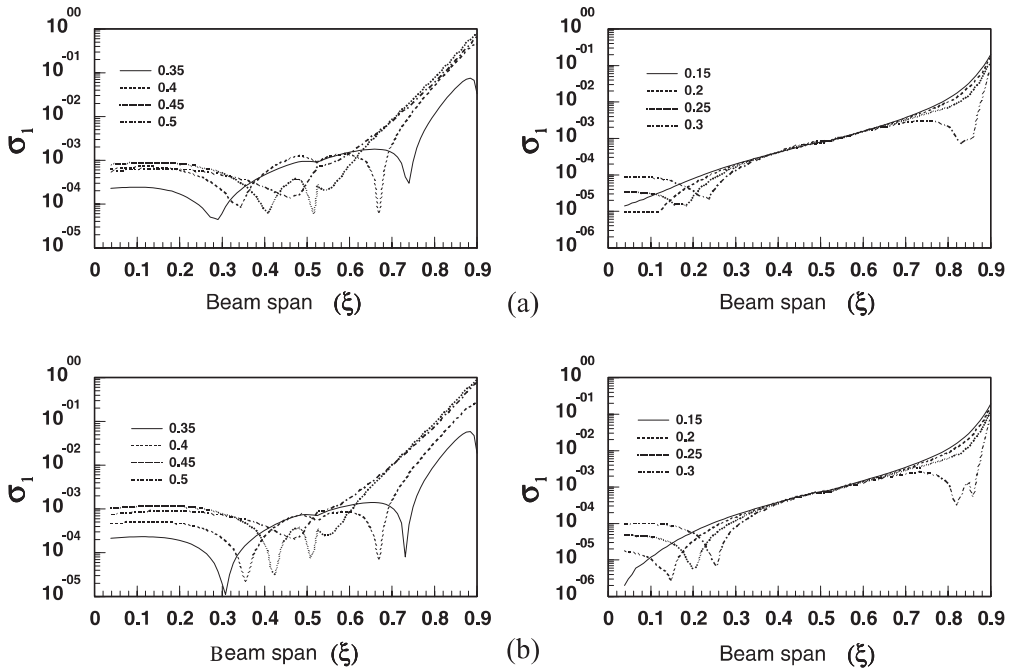
Figure 13. First mode distance function σ_1 (ξ) versus beam span (ξ) ($D = 0.3$): (a) using four rotational speeds ($\Omega = 1, 2, 3, 4$); (b) using three rotational speeds ($\Omega = 2, 3, 4$).

Table 1. Crack identification results ($D = 0.3$).

Used rotational speed	Actual	Crack location							
		0.15	0.2	0.25	0.3	0.35	0.4	0.45	0.5
1, 2, 3, 4		Fail	0.12	0.18	0.24	0.29	0.35, 0.67	0.41, 0.52	0.46
2, 3, 4	Predicted	0.04	0.15	0.2	0.26	0.31	0.35	0.43	0.47
2, 3		Fail	0.12	0.19	0.24	0.3	0.35	0.42	0.47
3, 4		0.08	0.17	0.22	0.32	0.32	0.36	0.43	0.47

values of the rotational speeds $\Omega = 2, 3, 4$, Figure 13b shows that the distance function σ_1 (ξ) has a clear global minimum. This minimum is used to predict the crack location for all cases. These locations are closer to the real locations than the previous prediction trial (using $\Omega = 1, 2, 3, 4$).

New prediction trials are shown in Figures 14a and 14b in which only two values of rotational speeds are used in each figure, namely $\Omega = 2, 3$ and $\Omega = 3, 4$, respectively. In both figures it can be seen that the distance function has a global minimum very close to the real crack location. A summary of predicted crack locations is given in Table 1.
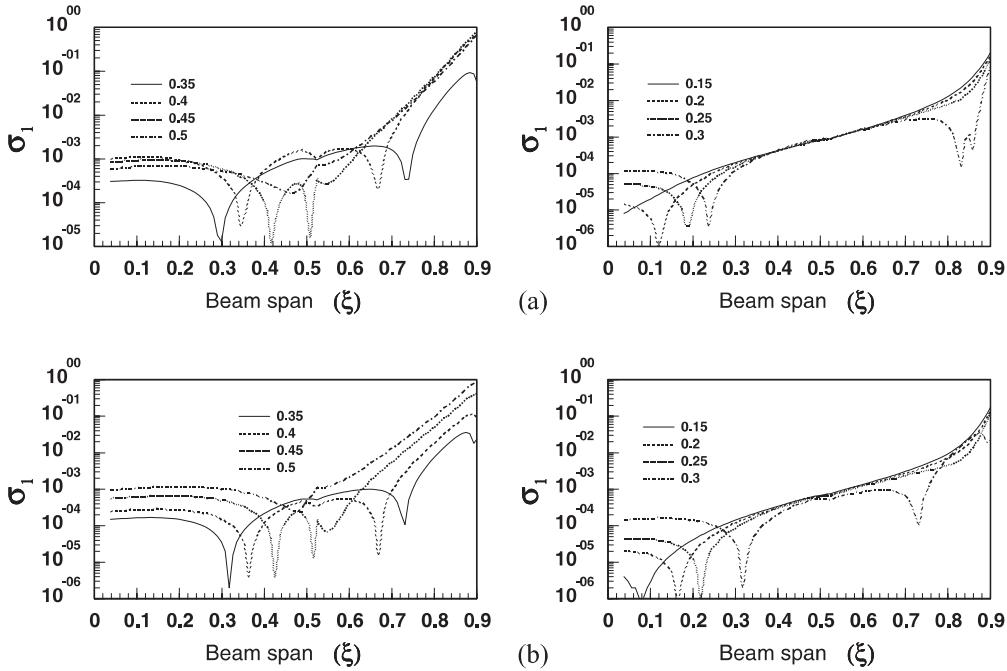
Figure 14. First mode distance function σ_1 (ξ) versus beam span (ξ) ($D = 0.3$): (a) using two rotational speeds ($\Omega = 2, 3$); (b) using two rotational speeds ($\Omega = 3, 4$).

6. CONCLUSIONS

A simple crack detection and localization algorithm for a rotating cracked Timoshenko beam has been proposed. The algorithm is based on a suggested mathematical model for the beam. It utilizes the variation of a single natural frequency due to a crack versus rotation speed to detect the crack location. The mathematical model that describes the lateral vibration of a rotating cracked Timoshenko beam has been derived using the assumed mode method and Lagrange's equations. This modeling approach globalizes the effects of the crack and the rotational speed. This is the case observed when experimentally measuring the frequency change due to a crack. The results from the mathematical model have been verified using a three-dimensional FEA. Good agreement has been observed between the theoretical results and those obtained from the FEA as well as good accuracy in localizing the crack. The suggested algorithm has built-in, multiple means of checking or confirming the crack analysis results it provides. This is due to the fact that independent analysis of the beam's health may be carried-out at different rotational speeds.

The localization algorithm shows promising capabilities in determining the location of a crack with good accuracy. Also, the algorithm has the capability to check/confirm its result by using different combinations of rotational speeds to calculate frequency variations.

REFERENCES

Al-Said, S. M., Naji M., and Al-Shukry, A. A., 2006, "Flexural vibration of rotating cracked Timoshenko beam," Journal of Vibration and Control 12(11), 1271–1287.

Chang, C.-C. and Chen, L.-W., 2004, "Damage detection of cracked thick rotating blades by a spatial wavelet based approach," *Applied Acoustics* **65**, 1095–1111.

Chasalevris, A. C. and Papadopoulos, C. A., 2006, "Identification of multiple cracks in beams under bending," *Mechanical Systems and Signal Processing* **20**, 1631–1673.

Cowper, G. R., 1966, "The shear coefficient in Timoshenko's beam theory," *Journal of Applied Mechanics Transaction of the ASME* **33**, 335–340.

Dimarogonas, A. D., 1996, "Vibration of cracked structures: a state of the art review," *Engineering Fracture Mechanics* **55(5)**, 831–857.

Doebling, S. W., Farrar, C. R., and Prime M. B., 1998, "A summary review of vibration-based damage identification methods," *The Shock and Vibration Digest* **30(2)**, 91–105.

Fang, X., Tang, J., Jordan, E., and Murphy, K. D., 2006, "Crack induced vibration localization in simplified bladed-disk structures," *Journal of Sound and Vibration* **291,** 395–418.

Huang, B.-W., 2006, "Effect of number of blades and distribution of cracks on vibration localization in a cracked pre-twisted blade system," *International Journal of Mechanical Sciences* **48**, 1–10.

Krawczuk, M., Palacz, M., and Ostachowicz, W., 2003, "The dynamic analysis of a cracked Timoshenko beam by the spectral element method," *Journal of Sound and Vibratio*n **264**, 1139–1153.

Kuang, J. H. and Huang, B. W., 1999, "The effect of blade crack on mode localization in rotating bladed disks," *Journal of Sound and Vibration* **227(1)**, 85–103.

Loya, J. A., Rubio, L., and Fernández-Sáez, J., 2006, "Natural frequencies for bending vibrations of Timoshenko cracked beams," *Journal of Sound and Vibration* **290**, 640–653.

Masoud, S., Jarrah, M. A., and Al-Maamory, M., 1998, "Effect of crack depth on the natural frequency of a pre-stressed fixed beam," *Journal of Sound and Vibration* **214**, 201–212.

Mei, C., Karpenko, Y., Moody, S., and Allen, D., 2006, "Analytical approach to free and forced vibrations of axially loaded cracked Timoshenko beams," *Journal of Sound and Vibration* **291**, 1041–1060.

Sung-Soo, K. and Ji-Hwan, K., 2003, "Rotating composite beam with a breathing crack," *Composite Structures* **60**, 83–90.

Tada, H., Paris, P. C., and Irwin, G. R., 2000, *The Stress Analysis of Cracks Handbook*, ASME Press, New York.

Wauer, J., 1990, "Cracked rotor dynamics: a state of the art survey," *Applied Mechanics Reviews* **43(1)**, 13–17.